Mon. Not. R. Astron. Soc. **288,** 1015–1021 (1997)

Keck high-resolution spectroscopy of Mrk 335: constraints on the number of emitting clouds in the broad-line region

Nahum Arav,[1]★ Tom A. Barlow,[2] Ari Laor[3] and Roger D. Blandford[1]

[1] *Theoretical Astrophysics, Caltech 130-33, Pasadena, CA 91125, USA*
[2] *Department of Astronomy, Caltech 105-24, Pasadena, CA 91125, USA*
[3] *Physics Department, Technion, Haifa 3200, Israel*

Accepted 1997 March 7. Received 1996 September 17

ABSTRACT

We present high-resolution (~ 6 km s^{-1}), high signal-to-noise ratio (~ 400 at Hα line centre) spectroscopy of Mrk 335. Cross-correlation (CC) analysis of the data yields a lower limit of $\sim 3 \times 10^6$ for the number of emitting clouds in the broad-line region (BLR) of this object. This limit is applicable for clouds with $T = 2 \times 10^4$ K and an optical depth of $\sim 10^4$ in their Hα line. The result is obtained from the absence of a CC signal in the data and from extensive Monte Carlo simulations that show the minimum number of clouds necessary in order to prevent the creation of a detectable CC signal. The simulations can be used to test any BLR model which is based on a contribution from discrete sources provided that the individual emission profile of the sources and their distribution are given. Current BLR models based on stellar atmospheres of bloated stars can be ruled out, unless the linewidth of an individual star exceeds 100 km s^{-1}. The lower limit on the number of emitting clouds also provides constraints on traditional photoionization models for a system of clouds.

Key words: techniques: spectroscopic – galaxies: individual: Mrk 335 – quasars: emission lines – galaxies: Seyfert.

1 INTRODUCTION

The origin of the broad emission lines (BELs) observed in many types of active galactic nuclei (AGN) remains unknown despite decades of dedicated research. The standard model assumes that the BELs are the product of emission from a large number of clouds moving with velocities of thousands of km s^{-1}. This picture arises from ionization considerations that require the existence of clouds with a filling factor $\sim 10^{-6}$ (e.g. Netzer 1990). Reverberation mapping observations exclude cloud motion in the form of a coherent inflow or outflow with respect to the central source (Maoz et al. 1991; Korista et al. 1995; but see Chiang & Murray 1996). The reverberation mapping also gives a rough estimate for the size of the broad-line region $r \sim 0.1 L_{46}^{1/2}$ pc, where L_{46} is the luminosity in units of 10^{46} erg s^{-1}.

Two models of clouds have been extensively studied in the literature. The first is the two-phase model in which cool clouds ($T \sim 10^4$ K) are embedded in a hot medium with $T \sim 10^8$ K (Krolik, McKee & Tarter 1981). The hot medium is needed in order to maintain the clouds in pressure equilibrium. Without this confining pressure the clouds will expand within a sound crossing time which is $\sim 10^7$ s for a typical cloud's parameters. This is much shorter than the dynamical time-scale for the cloud system (10^8–10^9 s), and would imply an unrealistic cloud creation rate. The origin of the clouds in this model is uncertain and the dynamics is problematic not least because the confining medium may destroy the clouds (Mathews & Ferland 1987). There are also difficulties in maintaining a two-phase equilibrium using a realistic AGN spectrum (Fabian et al. 1986; Mathews & Ferland 1987). A way around these difficulties is suggested by a second class of models which create the BELs out of stellar atmospheres or bloated stars (Scoville & Norman 1988; Kazanas 1989; Alexander & Netzer 1994; hereafter we refer to all these models as bloated star models). In these models the individual sources are slow (~ 10 km s^{-1}) outflows emanating from giant stars. The stars eliminate the need for an external confinement with all its associated difficulties. The number of bloated stars cannot be much larger than 10^5 in order to avoid an excessive

★E-mail: arav@tapir.caltech.edu

stellar collision rate and an unreasonable total number of stars in the cluster. Even with this number of bloated stars the collisional destruction rate is high and the resultant amount of mass which is injected into the local interstellar medium can be excluded observationally (Begelman & Sikora 1991). We also mention that it may be possible to confine the clouds magnetically (Rees 1987; Emmering, Blandford & Shlosman 1992).

One way to test such models, which are based on individual emitting units, is to search for a direct signature of the discrete clouds. The idea is to use cross-correlation (CC) techniques on high-resolution, high signal-to-noise ratio spectra of a bright AGN. The line profiles are fitted with a smooth function and the residuals (data − fit) of different lines, or of different observations of the same line are then cross-correlated. If any of the microstructure in the line profiles is a result of contributions from individual emitting clouds we should obtain a statistically significant CC signal at zero velocity shift. Existence of a CC signal can give a model-dependent estimate for the number of clouds that produce the line. A null result can be translated to a lower limit for the number of contributing clouds using Monte Carlo simulations. A simple version of this approach was used by Atwood, Baldwin & Carswell (1982) on a moderate resolution spectra of Mrk 509 and the lack of CC signal in their data was interpreted as a lower limit of 5×10^4 for the number of emitting clouds. The main significance of our result is the improvement on this limit by a factor of 100.

In this paper we derive the lower limit for the number of individual emitters based on high-resolution spectra taken with the Keck telescope, and contrast the results with the above models for BELs. The acquisition and reduction of the data is described in Section 2, the CC analysis in Section 3 and the Monte Carlo simulations which give the lower limit are described in Section 4. In Section 5 we derive an upper limit to the number of clouds based on simple photoionization arguments, and in Section 6 we discuss the implication of our results on the two-phase and bloated star models.

2 DATA ACQUISITION AND REDUCTION

The HIRES spectra for the Seyfert galaxy Mrk 335 were obtained during service observing with the Keck I telescope on 1995 September 11. The data consist of 2 exposures of 40 and 50 min (with cloudy skies and a full moon) each using a 0.86 arcsec slit (3 pixels) for a resolution of approximately 6.3 km s^{-1}. The actual resolution varies from about 6.0 to 6.5 km s^{-1} FWHM owing to the change in dispersion across each 4200 km s^{-1} wide echelle order. The wavelength coverage was 4720 to 7180 Å with some gaps beyond 500 Å. The signal-to-noise ratio per resolution element ranged from 100 in the continuum up to ~ 400 and ~ 150 for the Hα and Hβ emission lines, respectively. The wavelength calibration error is about 0.1 pixel (0.2 km s^{-1}) rms and up to a maximum error of about 0.3 pixel (0.6 km s^{-1}). This is the relative error across the spectrum, that is, the error in wavelength separation between two points in the spectrum. The absolute wavelength error is about 0.3 pixel (0.6 km s^{-1}), which is estimated from shifting the scale to night sky emission lines. So altogether there can be up to ~ 1 km s^{-1} error in the absolute wavelength value at any given pixel. As a result of imperfect corrections for variations in the pixel-to-pixel response (flat-field division), we estimate a fluxing error (defined as the deviation in the ratio of extracted counts to real counts) of about 0.5 per cent which appears to cause 'undulations' on the scale of several pixels. This is estimated from spectra of bright stars taken previously with HIRES. In addition, the process of combining different echelle orders introduces undulations in the spectrum of up to 3 per cent on scales of ~ 500 km s^{-1}. However, these do not significantly affect the results of our analysis, since we are interested in scales of ~ 50 km s^{-1} (see Sections 3 and 4).

The data were reduced using our own reduction package which automatically traces the orders, ignores anomalous radiation events, and uses an optimal weighting scheme similar to Horne (1986) for extracting the spectra, see Barlow (in preparation) for a description. In Fig. 1 we show the emission line data. Fig. 2 shows the Hα profile of the 50-min observation and superimposed on it the signal-to-noise ratio of the data.

3 CROSS-CORRELATION ANALYSIS

Fig. 1 shows that there are significant differences between the line profiles of Hα and Hβ. Therefore, it is possible that the clouds that give rise to most of the Hα emission are not the ones that give rise to most of the Hβ emission, and vice versa. If this is the case, a null CC signal between these two lines will be difficult to interpret. Furthermore, an individual cloud should have a different optical depth for Hα and Hβ which causes small differences in the intrinsic emission profiles for these lines within the cloud. A way to avoid these obstacles is to cross-correlate two different observations of the same line. Since the acquired data was already split into two similar length exposures (A and B) we decided to use this approach and to concentrate most of our effort on the Hα profile which has the higher signal-to-noise ratio.

The CC analysis was performed as follows: The continuum subtracted line profiles were fitted using eighth-order polynomials. A global fit for the whole profile did not work well owing to large systematic residuals. Therefore, we divided the full profile to subintervals and fitted them separately. In order to avoid large discontinuities at the edges of these intervals we averaged over 10 intervals which are shifted with respect to one another. This also gave us a more representative profile function. The χ^2 of the residuals divided by the errors was checked to be close to one in order to avoid both large systematic residuals (χ^2 significantly larger than 1) or too good a fit (χ^2 significantly less than 1).

We then calculated the CC function between the residuals of spectra A and B according to the following formalism:

$$\mathrm{CC}(\Delta v) \equiv \sum_{v} R_{\mathrm{A}}(v) R_{\mathrm{B}}(v + \Delta v), \qquad (1)$$

where $R_{\mathrm{A}}(v) \equiv \mathrm{flux}_{\mathrm{A}}(v) - \mathrm{fit}_{\mathrm{A}}(v)$ and with $R_{\mathrm{B}}(v)$ similarly defined. Since we are only interested in the relative magnitude of CC(0) we did not normalize the function. A typical CC(Δv) is shown in Fig. 3. We tested many different combinations of fitting parameters and found that the exact

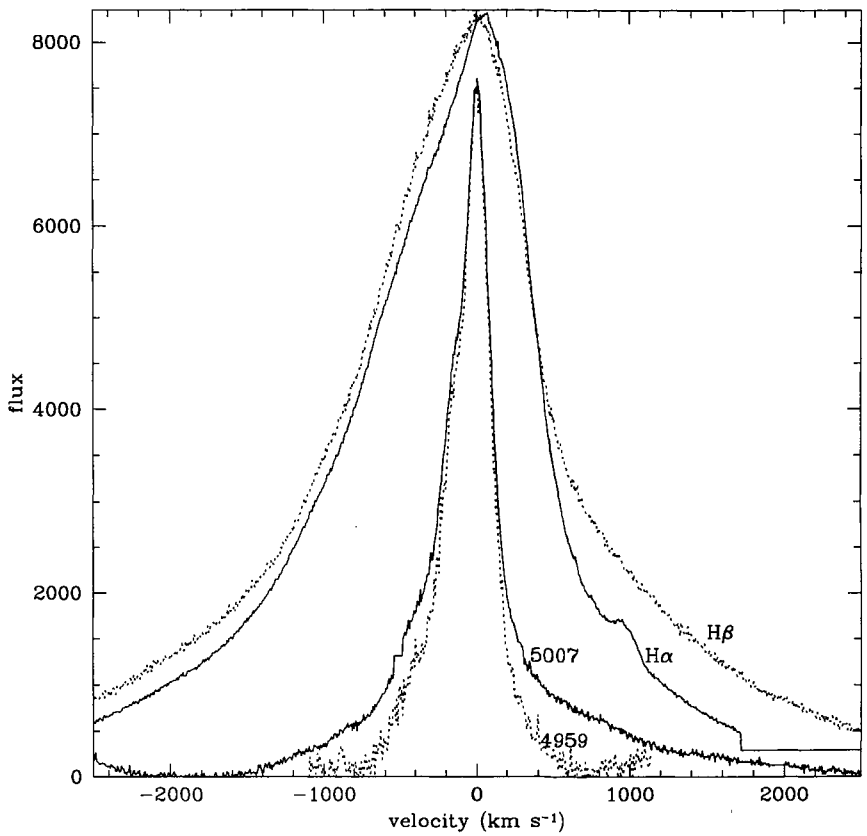

Figure 1. The observed line profiles of Mrk 335 (continuum subtracted) in arbitrary scaling that matches the peaks of Hα and Hβ, and separately the peaks of the O III lines (5007 and 4959 Å). The profiles of the 5007 and 4959 Å lines do not match owing to blending with Hβ.

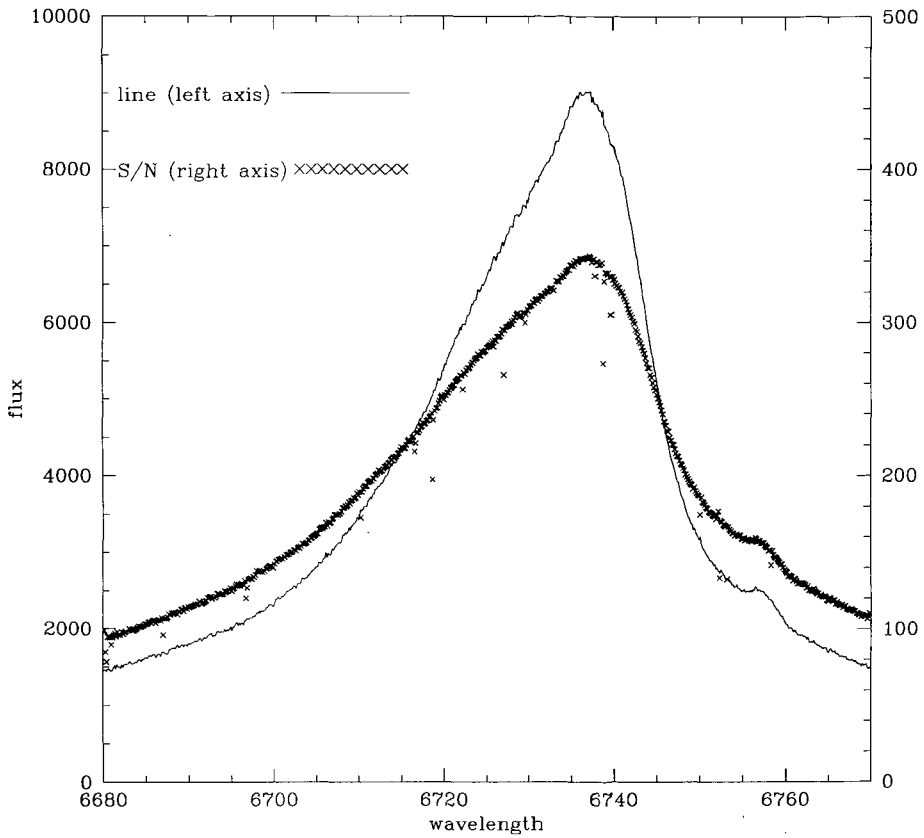

Figure 2. The 50-min observation of the Hα line (flux in arbitrary units) and superimposed on it the signal-to-noise ratio of the data.

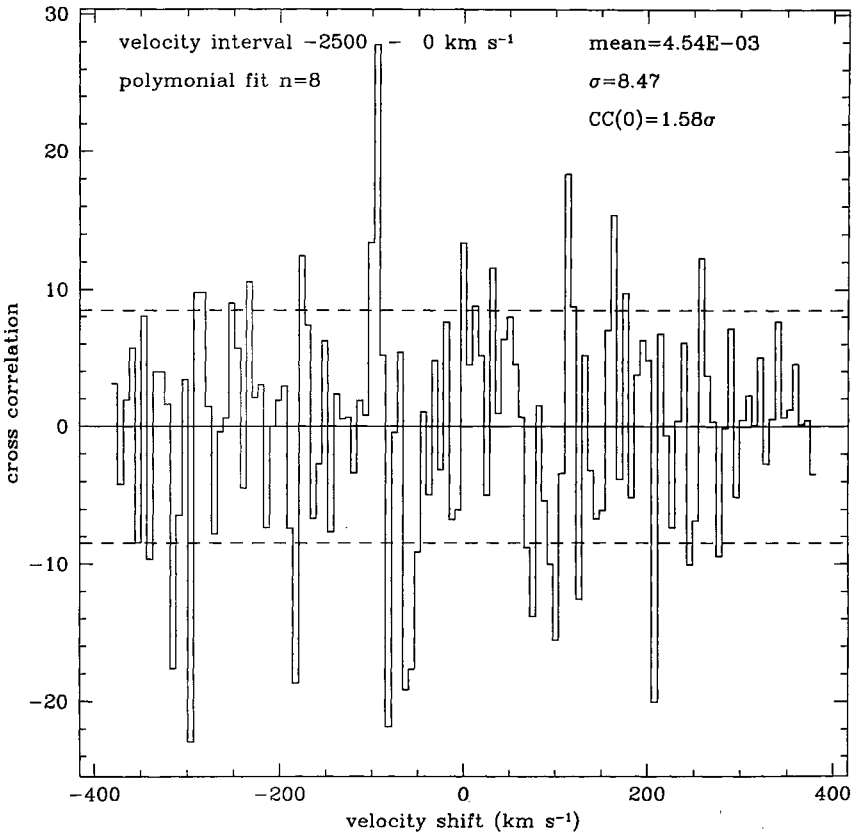

Figure 3. The cross-correlation (CC) function for the residuals of $H\alpha_A$ and $H\alpha_B$ (see equation 1). No significant CC value is seen at zero velocity shift. The histogram is the CC function and the dashed lines are $\pm 1\sigma$, CC(0) is the value of the function at zero velocity shift in σ units.

degree of the fitting polynomial did not make any substantial difference provided it was five or higher. The length of the subintervals had to be kept between 80 and 150 resolution elements (500–1000 km s^{-1}) in order to obtain residuals with a reduced χ^2 around 1, but within this range, the CC function did not change qualitatively with changes in the length of the subintervals. We used different subintervals for the fitting of spectra A and B in order to avoid systematic effects from identical fitting procedure. We tried Gaussian smoothing the CC function with velocity widths appropriate to physical clouds (20–50 km s^{-1}) in order to enhance the CC on these scales. The same analysis was repeated for the Hβ of the two spectra, and for the Hα and Hβ in the combined spectrum. The end result is that there is no significant CC signal in the data around zero velocity shift.

4 MONTE CARLO SIMULATIONS

In order to translate the null result of the CC analysis to an upper limit on the number of clouds we performed extensive Monte Carlo simulations. The simulations were designed to resemble the actual CC analysis as closely as possible.

To simulate a line profile made of individual cloud contributions combined with realistic noise we used the following approach. Smooth templates for the line profiles were obtained by using the fitting procedure described above, that is, each velocity-resolution element is assigned a flux value. A random integer number N is generated in the interval between 0 and k_0, where k_0 is the number of velocity-resolution elements in the extracted profile, with equal probability inside that interval. This number is used as an indicator for the velocity position. A second random number M is generated with equal probability between zero and twice the peak flux in the template. If M is smaller than the flux at velocity position N a cloud is added at that velocity position. The process is repeated a large number of times until the desired number of contributing clouds is reached. To zeroth order, the number of clouds in each bin N is proportional to the flux value of the template at that bin. However, the actual number of clouds in each bin deviates randomly from exact proportionality to the flux value. More precisely, the number of clouds in bin N is normally distributed around cF_N where F_N is the flux level of the extracted profile at resolution element N and c is the proportionality constant. To simulate thermally emitting clouds we multiply the numerical value of each bin by $\exp[-v^2/b^2]$ centred on that bin and allow it to contribute to neighbouring bins. To make the velocity distribution less rigid, each bin was divided into 10 subintervals with each new point assigned the appropriate template extrapolated flux level. A similar profile simulation ensued and finally the emission in 10 sub-bins was added to regain the original number of resolution elements.

For producing random noise we use the same method without multiplying by a Gaussian function and without

changing the number of bins. The residuals of this process are normally distributed along the profile template, and thus have the characteristic of photon shot noise. The number of iterations for noise generation was chosen to match the signal-to-noise ratio in the data. The synthetic noise mimics the actual noise quite well since the latter is dominated by photon shot noise. The simulated noise is added to the cloud-simulated line profile. A second profile is produced by adding an independently generated noise to the same cloud-simulated line profile. There are now two line profiles made up from the same underlying cloud distribution, but with different random noise.

We then use the same algorithm that was used on the real data to calculate the CC function, where we apply Gaussian smoothing over the velocity width b of the simulated clouds. A positive result is defined as a 3σ signal at zero velocity shift. The parameter phase space for the simulations was thoroughly probed: number of clouds, Gaussian width of clouds and length of fitting intervals for either line. The results show that for a homogeneous cloud population with emission given by a thermally broadened Gaussian with a 20 000 K temperature ($b = 18$ km s^{-1}), more than 10^7 clouds are needed in order not to detect a positive CC signature. When we use clouds with a realistic $\tau_{H\alpha} = 10^4$ (Rees, Netzer & Ferland 1989) the lower limit on the number of clouds is 3×10^6 (see Fig. 4). For $b > 80$ km s^{-1} the success of the fitting procedure in finding the correlated residuals diminishes rapidly, since it effectively smooths features on scales larger than 100 km s^{-1}. The reason for the smaller lower limit in the case of the large $\tau_{H\alpha}$ is that the emission is effectively broadened by $\sqrt{\ln \tau}$ (Davidson & Netzer 1978), which for the above $\tau_{H\alpha}$ value yields a factor of 3 broadening. Wider Gaussians are harder to detect because the fluctuations they cause are smoothed over a larger velocity range. The actual emission of an optically thick cloud deviates from a simple broad Gaussian, since a considerable part of the emission should come from the wings of the line where the optical depth is close to unity. In order to mimic such a behaviour we ran simulations where the emission profile is in the shape of two adjacent Gaussians separated by $\sim b$ km s^{-1}. Using such a profile made only small changes in the simulations, so for the sake of simplicity we opted to use pure Gaussians. Fig. 5 shows the CC($\Delta v = 0$) as a function of b for different number of clouds. As expected the CC($\Delta v = 0$) diminishes when broader individual emission profiles are used.

As we mentioned in Section 1, the lower limit for the number of individual emitting clouds in Mrk 335 can be used to constrain theoretical models of the BLR that are based on emission from discrete sources. Models which are based on non-discrete emission (i.e., disc emission, emission from continuous flow) are compatible with our result, since they are expected to have no CC signal. Any detailed model for the creation of the BELs from discrete emitting units can be tested using our Monte Carlo simulations. In order to do so the emission profile of individual sources and their relative flux contribution should be given. Using these parameters the simulation can immediately give the mini-

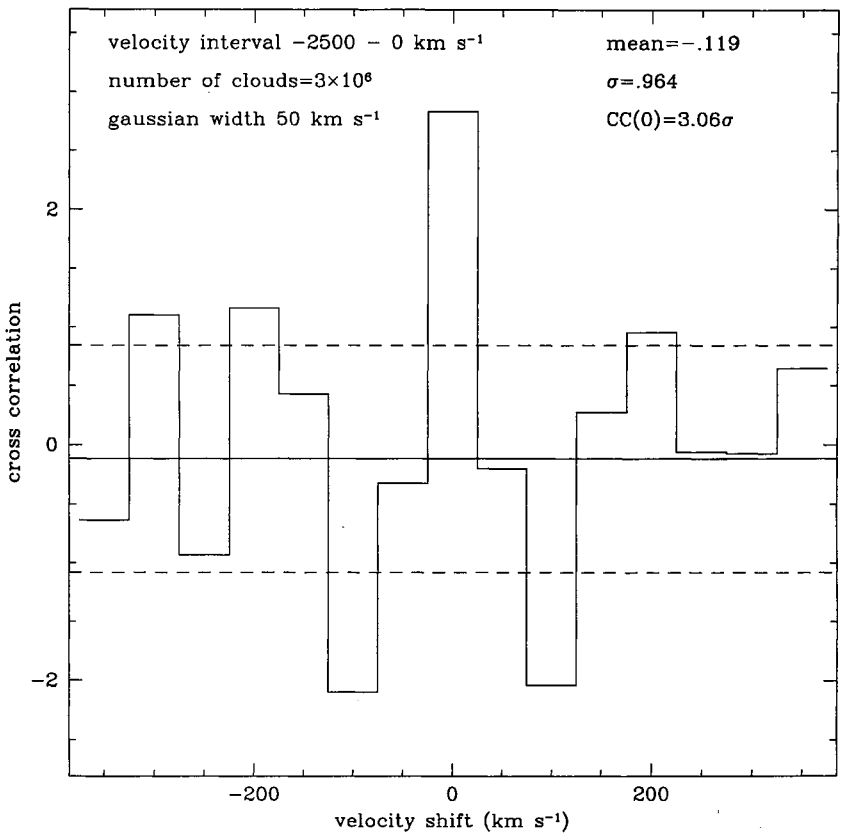

Figure 4. Similar to Fig. 3 for simulated line spectra, except that the CC was smoothed on a scale corresponding to the width of the clouds. It is evident that a strong CC signal should be detected at zero velocity shift if the lines are made of 3×10^6 clouds.

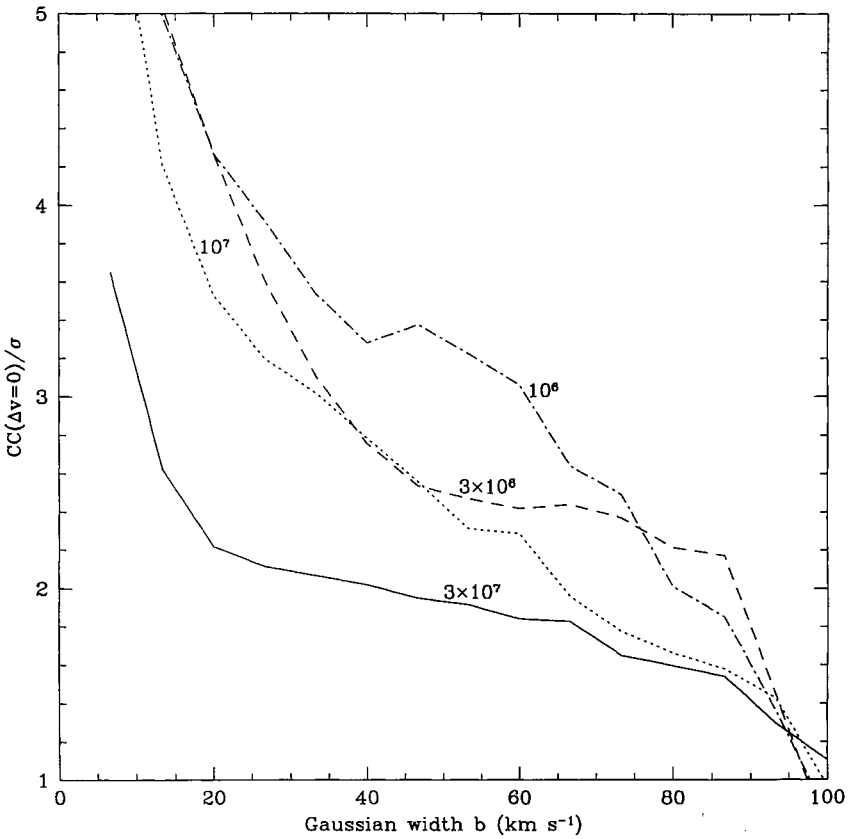

Figure 5. The dependence of CC($\Delta v=0$) on the emission-width of individual clouds. The number that labels each curve is the number of clouds used in the simulation. Each curve represents one combination of clouds and noise where only the velocity width of the clouds is changing. The general trend of higher CC($\Delta v=0$) for smaller number clouds at a given width is evident.

mum number of such sources that is consistent with no CC signal.

5 NUMBER OF CLOUDS FROM PHOTOIONIZATION CONSIDERATIONS

Theoretical estimates for the number of clouds in the BLR can be obtained from photoionization models using the following physical parameters.

(i) The size of the BLR $R_{\rm BLR}$. As indicated by reverberation mappings of both Seyfert 1 galaxies (Peterson 1993) and quasars (Maoz 1997), the size of the BLR is consistent with $R_{\rm BLR}=0.1L_{46}^{1/2}$ pc (where L_{46} is the luminosity of the AGN in units of 10^{46} erg s^{-1}). This scaling is also naturally explained by dusty photoionized gas models (Netzer & Laor 1993).

(ii) The thickness of each cloud in the BLR, l. The photoionized column of a slab of gas, $\Sigma_{\rm ion}=ln_{\rm e}$ (where $n_{\rm e}$ is the electron number density), can be estimated by equating the number of recombinations per unit cloud area to the flux of ionizing photons per unit area, which gives $\Sigma_{\rm ion}=10^{23}U$, where $U=n_\gamma/b_{\rm e}$ is the ionization parameter and the density of ionizing photons is $n_\gamma=6.6\times10^{55}L_{46}/4\pi r^2c$ cm^{-3} (Laor & Draine 1993, where r is the distance from the emitter and c is the speed of light). The high-ionization lines (e.g. C IV λ1549, N V λ1240) are formed within $\Sigma<\Sigma_{\rm ion}$ of the illuminated cloud surface, while low-ionization lines (e.g. Mg II λ2798) require $\Sigma\sim3$–$10\Sigma_{\rm ion}$. The Hα and Hβ lines discussed in this paper are also produced mostly within the extended partially ionized zone, i.e. within $\Sigma\sim10\Sigma_{\rm ion}$ (e.g. Netzer 1990). The Balmer line flux from the highly ionized layer is close to the 'classical' Balmer/Lyman recombination line ratio (e.g. Osterbrock 1989), which is 3–5 times smaller than typically observed. Collisional excitations strongly enhance the Balmer line flux within the partially ionized region, and may explain the large enhancement observed in the Balmer/Lyman line fluxes.

(iii) The covering factor of the BLR clouds, $C_{\rm BLR}$. This parameter can be estimated by comparing the number of H-ionizing photons produced by the central continuum source to the number of Lyα photons, which is a measure of the number of ionizing photons absorbed in the BLR. The typical value in AGNs is $C_{\rm BLR}\sim0.1$ (Netzer 1990).

If the BLR is composed of spherical clouds of radius $r_{\rm c}$, with a mean thickness $l=4/3r_{\rm c}$, then the number of clouds in the BLR is $N_c=C_{\rm BLR}4\pi R_{\rm BLR}^2/\pi r_{\rm c}^2$. For clouds which produce Hα and Hβ we assume $\Sigma=10\Sigma_{\rm ion}$. Substituting the expressions for $r_{\rm c}(U,n_{\rm e})$ and $R_{\rm BLR}(L_{46})$ we get $N_c=6.4\times10L_{46}n_{10}^2U_{0.1}^{-2}$, where $n_{\rm e}=10^{10}n_{10}$ cm^{-3} and $U=0.1U_{0.1}$. The density and ionization parameter are related through $U=0.2L_{46}r_{0.1}^{-2}n_{10}^{-1}$, which using the $R_{\rm LBR}(L_{46})$ relation gives $U_{0.1}=2n_{10}^{-1}$ in the BLR. Thus, we get $N_{\rm c}=2.5\times10^9L_{46}U_{0.1}^{-4}$. In the case of Mrk 335 $f_\lambda=6\times10^{-14}$ erg cm^{-2} s^{-1} at 1500 Å which, using a bolometric correction

factor of 5 (e.g. fig. 7 in Laor & Draine 1993) and $H_0 = 75$ km s^{-1} Mpc^{-1}, gives $L_{46} = 0.05$. Thus, for $U = 0.1$ we expect $\sim 10^8$ clouds in the BLR of Mrk 335. Netzer (1990) performed a similar analysis using a somewhat harder X-ray spectrum. Extrapolating his estimate to the case of Mrk 335 we obtain $N_c \sim 10^7$. The difference between the two estimates is mainly due to the larger Σ that is needed for a harder spectrum.

The estimate made above assumes a single type of cloud (i.e. a given n and U) and a single value for $R_{\rm BLR}$. Reverberation mappings indicate that different lines originate at a range of distances (Peterson 1993), and the strength of high-ionization lines, such as O VI λ1034, indicates that a range of U values must also be present in the BLR. Thus, the value of U in the Balmer line emitting clouds is rather uncertain, and since $N_c \propto U^{-4}$, the actual number of clouds may be off by two orders of magnitude or more in either direction from the estimates given above.

6 DISCUSSION

Our current result puts strong constraints on the bloated star models. As a result of the low invoked wind velocity, the emission profile from an individual bloated star can be approximated as a Gaussian with a width of around 50 km s^{-1}. Therefore, our lower limit for the number of emitting clouds is higher by at least a factor of 30 than the largest allowed number of such stars. This is enough to exclude the current version of these models. We note that in Mrk 335 the number of contributing stars must be much smaller that 10^5 since the size of its BLR is about an order of magnitude smaller than that of a typical bright quasar, for which this limit holds.

A possible way to amend the bloated star models in a way that will make them consistent with the null CC result is to assume much higher wind velocities (which might be caused by radiative pressure from the quasar itself; Arav, Li & Begelman 1994; Scoville & Norman 1995). This might make the individual stellar emission broad enough to make the lower limit of the CC simulations consistent with 10^5 ($b > 100$ km s^{-1}). However, it might be that the bulk of emission would still come from the low-velocity region of the wind (because of its higher density). Furthermore, with higher wind speed the bloated star models may have difficulties with other aspects of creating realistic BELs, such as producing broad [O III] $\lambda\lambda$ 4959, 5007 lines (Alexander & Netzer 1994).

Looser constraints can be put on the generic confined cloud model. The number estimate we derived from photoionization considerations (see Section 5) can be used as a rough upper limit since it is based on the size of the smallest cloud that is compatible with the observed strength of BEL in AGNs. If larger clouds are used the number of clouds that are needed to cover 10 per cent of the source is obviously smaller. The same is true for clouds with a distribution of radii, since fewer are needed to cover the source than in the case where all clouds have the minimum radius. The case of different radii should also lead to a stronger CC signal owing to the larger clouds, and thus the lower limit on the number of emitting clouds from the simulations becomes larger.

The lower limit of $\sim 10^7$ clouds in the BEL region of Mrk 335 is within the limits of the photoionization estimate (e.g. 10^7–10^8). However, the estimate is based on the smallest allowable clouds. A BLR composed of such clouds appears physically unappealing. There is no obvious physical mechanism which can form such a large number of small clouds, or confine these clouds once they are formed (e.g. Mathews & Ferland 1987). It now appears that there is no reliable upper limit on the column density in the BLR (as was claimed in the past; Ferland & Persson 1989). Thus the BLR clouds need not necessarily have a width comparable to the thickness of the photoionized layer. One might speculate that the BLR emission arises from the photoionized surface of a much smaller number of large clouds, possibly molecular clouds (which are detected in the narrow-line region). The lower limit on N_c and the general method provided in this paper serve as a significant constraint for such models.

ACKNOWLEDGMENTS

We thank Tom Bida for acquiring these observations and S. Vogt for leading the construction of the HIRES spectrograph. NA and RDB acknowledge support from NSF grants 92-23370 and 95-29170. AL acknowledges support from the E. and J. Bishop research fund, and from the Milton and Lillian Edwards academic lectureship fund.

REFERENCES

Alexander T., Netzer H., 1994, MNRAS, 270, 803
Arav N., Li Z. Y., Begelman M. C., 1994, ApJ, 432, 62
Atwood B., Baldwin J. A., Carswell R. F., 1982, ApJ, 257, 559
Begelman M. C., Sikora M., 1991, in Holt S. S., Neff S. G., Urry C., eds, Proc. AIP Conf. 254, Testing the AGN Paradigm. AIP, New York, p. 568
Chiang J., Murray N., 1996, ApJ, 466, 704
Davidson K., Netzer H., 1978, Rev. Mod. Phys., 51, 737
Emmering R. T., Blandford R. D., Shlosman I., 1992, ApJ, 385, 460
Fabian A. C., Guilbert P. W., Arnaud K., Shafer R. A., Tennant A. F., Ward M. J., 1986, MNRAS, 218, 457
Ferland G. J., Persson S. E., 1989, ApJ, 347, 656
Horne K., 1986, PASP, 98, 609
Kazanas D., 1989, ApJ, 347, 74
Korista K. T. et al., 1995, ApJS, 97, 285
Krolik J. H., McKee C. F., Tarter C. B., 1981, ApJ, 249, 422
Laor A., Draine B. T., 1993, ApJ, 402, 441
Maoz D., 1997, in Peterson B. M., Cheng F.-Z., Wilson A. S., eds, ASP Conf. Ser. Vol. 113, Emission Lines in Active Galaxies: New Methods and Techniques. Astron. Soc. Pac., San Francisco, p. 138
Maoz D. et al., 1991, ApJ, 367, 493
Mathews W. G., Ferland G. J., 1987, ApJ, 323, 456
Netzer H., 1990, in Blandford R. D., Netzer H., Woltjer L., eds, Saas-Fee Advanced Course 20: Active Galactic Nuclei. Springer, New York, p. 57
Netzer H., Laor A., 1993, ApJ, 404, L51
Osterbrock D. E., 1989, Astrophysics of Gaseous Nebulae and Active Galactic Nuclei. University Science Books, California
Peterson B., 1993, PASP, 105, 247
Rees M. J., 1987, MNRAS, 228, 47P
Rees M. J., Netzer H., Ferland G. J., 1989, ApJ, 347, 640
Scoville N., Norman C., 1988, ApJ, 332, 162
Scoville N., Norman C., 1995, ApJ, 451, 510